Optimal Analog-to-Digital Converter Resolution on Current Control for Precise Positioning Control

Hongzhong Zhu*, Hiroshi Fujimoto (The University of Tokyo)

Abstract

Current control for precise positioning control requires accurate current signals. However, current measurement error including current metering error and quantization error is unavoidable in digital control. In this paper, an approach of determining the optimal resolution of A/D converter to reduce the quantization effects is presented by taking into account the statistical properties of the current metering error. The effectiveness of the proposed method is verified by experiments using a high-precision stage.

Key words: current measurement, quantization, dither, analog-to-digital converter, current control

1. Introduction

Precise current measurement is essential for current control and sensorless control to produce high static and dynamic performance of ac motor drive systems. As the current measurement error is introduced into the control system by current sensors and analog-to-digital converters, the real current signals of a motor are not guaranteed to follow the reference values even when the measured current can follow them exactly. This would cause torque ripple and deteriorate the control performance especially at low load [2] [3]. Therefore, understanding and suppressing the current measurement error have attracted a great deal of attention [1] [4] [5].

Current measurement error can be classified into the metering error and the quantization error. The metering error, which is caused by thermal drift, dc offset and scaling inaccuracy, is introduced into control loop by current sensors and other analog devices in the measuring system. The quantization error arises because the analog current signal may assume any value within the input range of the A/D converter while the output data is a sequence of finite precision samples. Quantization error behaves as highly colored noise and cannot be ignored in many cases. For example, it is reported that quantization error can affect the accuracy of the motor position estimation for sensorless control when high frequency signal injection method is used [4].

It is known that white noise is easier to deal with than other colored noise because it contains equal power at any center frequency. Many methods, such as Kalman filter and LQG controller design methods, are studied based on the assumption that the noises introduced to the system are white. Motivated by this perspective, in this paper, dithering techniques are applied to analyze the effects of current measurement error. Dither, which is an intentionally applied form noise, can decorrelate signal-dependent noise, has been actively researched to suppress the quantization effects on audio or video signal processing [6] [7]. It is indicated that by treating the current metering error as a sort of dither, the quantization error can be whitened if a proper resolution of A/D converter is applied.

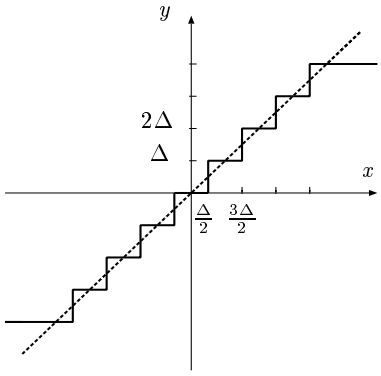

Fig. 1. Quantization characteristic. Δ is the quantization step.

The remainder of this paper is organized as follows. Section 2 presents some important theorems referring to quantization and dither. The current measurement is analyzed and the approach of determining the optimal resolution of A/D converter is presented in Section 3. Section 4 demonstrates the effectiveness of the approach via experiments. Finally, conclusion is given in Section 5.

2. Preliminaries

2.1 Quantization An ideal A/D converter is a nonlinear device having a staircase-type I/O relation, as shown in Fig. 1. The amplitude of an input signal is arbitrary and the possible amplitude of output signal is countably finite number of values. Assuming that the input is always within the measurement range of A/D converters, the converter can be expressed in terms of the input x and the quantization step Δ as

$$Q(x) = \Delta \lfloor \frac{x}{\Delta} + \frac{1}{2} \rfloor, \quad \cdots\cdots (1)$$

where $Q(\cdot)$ is denoted as the quantizing operation. The quantization error is defined by

$$q \triangleq y - x$$

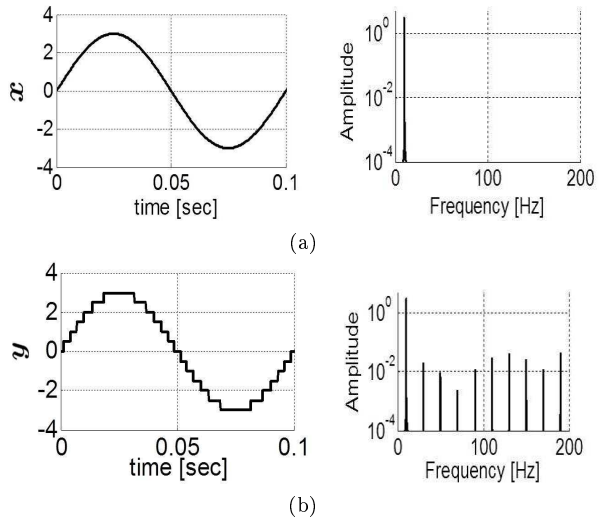

Fig. 2. Example of quantization feature. (a) shows the input signal and its frequency characteristic, (b) shows the quantized output signal and its frequency characteristic.

$$= Q(x) - x, \quad \cdots\cdots (2)$$

where y is the output. q is dependent of x unless x satisfies the so-called band-limited condition, which is also referred to as the "Quantization Theorem" [10]. The band-limitedness assumption on the input is not satisfied universally. Generally, the quantization error is dependent of input x. Although q is usually highly colored, its classical model treats it as a random process with a probability density function (pdf)

$$p_q(\epsilon) = \begin{cases} \frac{1}{\Delta}, & -\frac{\Delta}{2} < \epsilon \leq \frac{\Delta}{2} \\ 0, & \text{otherwise.} \end{cases} \quad \cdots\cdots (3)$$

Based on this kind of treatment, the mean and the variance of the quantization error are [7]

$$E[q] = 0, \quad \cdots\cdots (4)$$

$$E[q^2] = \frac{\Delta^2}{12}. \quad \cdots\cdots (5)$$

This treatment is valid for complex input signals whose amplitudes are large compared to the quantization step Δ. It fails catastrophically for small or simple signals. The quantization feature of an ideal A/D converter with the quantization step $\Delta = 0.5$ is shown in Fig. 2. Fig. 2(a) shows the sine wave input signal (left) and its frequency characteristic (right), and Fig. 2(b) shows the quantized output signal (left) and its frequency characteristic (right). From the frequency characteristic of quantized output, it is observed that many sharp peaks fall at multiples of the input sine wave frequency, indicating a strong correlation between the quantization error and the system input.

2.2 Dither Dither, which is an intentionally applied form noise and can decorrelate signal-dependent noise, has been wildly applied in the past fifty years to suppress the quantization effects on audio or video signal processing [6] [7] [11]. There exist two archetypes of dithering systems: subtractively dithered system and nonsubtractively dithered system. Schematics of these systems are shown in Fig. 3. In the subtractively dithered system, the total error is given by

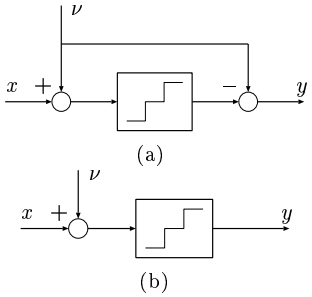

Fig. 3. Dithering systems. (a) Subtractively dithered system; (b) Nonsubtractively dithered system. x is the system input, and y is the system output.

$$\begin{aligned} e &= y - x \\ &= Q(x+\nu) - (x+\nu) \\ &= q(x+\nu), \end{aligned} \quad \cdots\cdots (6)$$

where ν denotes the dither. As reported in [6], the statistical properties of the dither ν can be chosen to control the properties of the total error e without increasing its variance. However, the requirement of synchronous dither subtraction at the system output cannot always be implementable in practical situations. It is for such reason, nonsubtractively dithered technique introduced in the following is of interest.

In the nonsubtractively dithered system, the total error e can be expressed by

$$\begin{aligned} e &= y - x \\ &= Q(x+\nu) - x \\ &= q(x+\nu) + \nu. \end{aligned} \quad \cdots\cdots (7)$$

The total error is not simply the quantization error, but also involves the dither. It is shown that the following result can be obtained [7]:

Theorem: In an nonsubtractive dithering system, $E[e^l|x]$ is independent of the distribution of the input x for $l = 1, 2, ..., M$ if and only if the characteristic function of the dither, P_ν, satisfies the condition that

$$\frac{d^i P_\nu}{d\,u^i}(u)\,\Big|_{u=k/\Delta} = 0 \quad \text{for } k = \pm 1, \pm 2, \pm 3, ..., \quad \cdots\cdots (8)$$

where $i = 0, 1, 2, ..., M-1$. The characteristic function of a random variable is the Fourier transform of its probability density function, which is defined by

$$P_\nu(u) \triangleq \int_{-\infty}^{\infty} p_\nu(\epsilon) e^{-j2\pi u\epsilon} d\epsilon. \quad \cdots\cdots (9)$$

Based on this theorem, the moments of the total error is shown as follows:

$$E[e] = E[\nu], \quad \cdots\cdots (10)$$

$$E[e^2] = E[\nu^2] + \frac{\Delta^2}{12}, \quad \cdots\cdots (11)$$

$$E[e^m] = \sum_{l=0}^{\lfloor m/2 \rfloor} \binom{m}{2l} \left(\frac{\Delta}{2}\right)^{2l} \frac{E[\nu^{m-2l}]}{2l+1}, \quad \cdots\cdots (12)$$

where $m = 1, 2, ..., M$.

It is shown in [8] that triangular-pdf dither of 2-LSB peak-to-peak amplitude

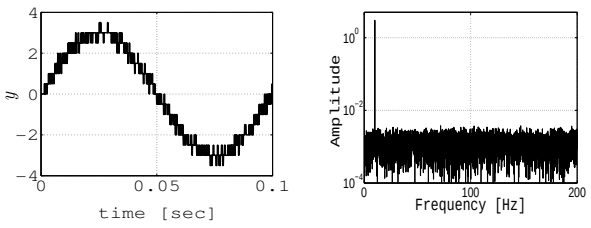

Fig. 4. The output signal by applying nonsubtractive dither technique and its frequency characteristic.

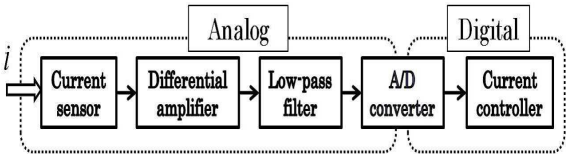

Fig. 5. Path of current measurement.

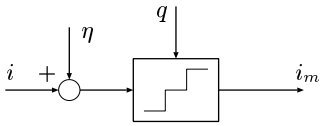

Fig. 6. Model of the current measurement: η is the metering error, and q is the quantization error.

$$p_\nu(\epsilon) = \begin{cases} \frac{1}{\Delta^2}(\epsilon + \Delta), & -\Delta < \epsilon \leq 0 \\ \frac{1}{\Delta^2}(-\epsilon + \Delta), & 0 < \epsilon \leq \Delta \\ 0, & otherwise, \end{cases} \quad \cdots\cdots\cdots (13)$$

is unique and optimal in the sense that it renders the total error be spectrally white while minimizing its second moment error $E[e^2]$. According to calculation, the mean and the variance of a dither with the triangular-pdf (13) is

$$E[\nu] = 0, \quad \cdots\cdots\cdots (14)$$

$$E[\nu^2] = \frac{\Delta^2}{6}. \quad \cdots\cdots\cdots (15)$$

Therefore, the mean and the variance of the total error e are

$$E[e] = 0, \quad \cdots\cdots\cdots (16)$$

$$E[e^2] = \frac{\Delta^2}{4}. \quad \cdots\cdots\cdots (17)$$

Fig. 4 shows the results of applying nonsubtractive dithering technique. The input signal and the quantization step are the same as the signal shown in Fig. 2(a). The aforementioned triangular-pdf dither (13) is used. From the figure of frequency characteristic, Surprising as it may seem, the output signal sounds like to be composed of the ideal input signal and a constant white noise. The results should be compared with those in Fig. 2.

3. Analysis of Current Measurement

In this section, firstly, the current measurement for digital current control is analyzed. Then, the dithering techniques presented in the previous section are applied to determine the optimal resolution of A/D converters.

Fig. 5 shows the typical path of the current measurement [12]. Currents, transduced to the voltage signal by current sensors, are transformed into digital values via A/D converters after amplitude amplification and noise filtering. During this procedure, the metering error and the quantization error are introduced to the control system. The block diagram of current measurement is shown in Fig. 6. The metering error, denoted by η, is caused by thermal drift, dc offset and scaling inaccuracy of the analog devices. The quantization error arises because of A/D converters is applied as converting analog signal to digital signal. Without loss of generality, the real current value is assumed to be within the measuring range of current sensors, which means that the metering accuracy is guaranteed. The quantization step Δ can be defined by

$$\Delta = \frac{I_0}{2^{N_b - 1}}, \quad \cdots\cdots\cdots (18)$$

where the measurement range of current sensor is set as $\pm I_0$, and N_b is the resolution of an A/D converter. Based on the nonsubtractive dither theory, it is easy to come out that the metering error should have positive effects on reducing the quantization effects caused by A/D converters. The following **Proposition** is achieved:

Proposition: Suppose that the metering error η is zero-mean and its probability density function is a triangular-pdf with the variance of V, the optimal resolution of the corresponding A/D converter in the sense of achieving independent measurement error is

$$N_b = \left[\log_2 \frac{I_0}{\sqrt{6V}} + 1\right], \quad \cdots\cdots\cdots (19)$$

where $[\cdot]$ means the operation of round-off.

This is easy to be proved from the perspective of adjusting the quantization step Δ to "fit" the metering error η so that the quantization noise can be whitened.

It will be illustrated in next section that the distribution of the metering error η can be approximated to triangular-pdf noise in practical situation. In addition, it is reported in [9] that a noise with Gaussian distribution is also effective on suppressing the quantization effects.

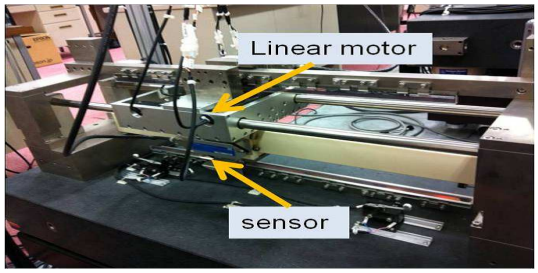

Fig. 7. The experimental setup.

Table 1. Parameters of stage

Inductance L	6.4×10^{-3}	H
Resistance R	13.1	Ω
Mass M	14.3	kg
Viscosity B	24	$N/(m/s)$
Thrust coefficient K_t	26.5	N/A
Bach-EMF constant K_e	9.5	$V/(m/s)$

4. Experiments

In this section, the method of determining optimal A/D

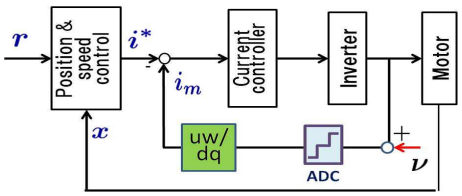

Fig. 8. Block diagram of control system.

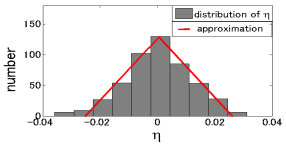

Fig. 9. Histogram plot of the metering error by using an A/D converter with the resolution of 14-bit.

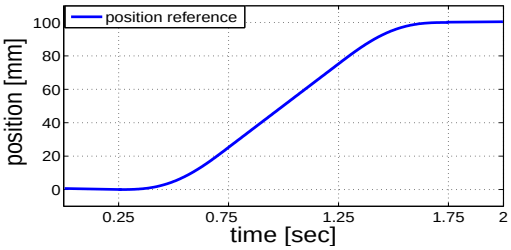

Fig. 10. Position reference.

converters from the viewpoint of dither techniques are verified via experiments by using a high-precision stage. The experimental setup is shown in Fig. 7, whose parameters are shown in Table. 1. The stage is driven by linear motors and the position information is measured by linear encoder with the resolution of 1 nm. U-phase and W-phase currents are measured by FA-050PV with the range of $\pm I_0 = \pm 50$A. The A/D converters whose resolution is 14-bit is exploited. VSPTC with SRC method [13] is used to design position&speed controllers to generate current reference. Vector control method is applied for current control and pole-zero cancellation controller is used. The block diagram of control system is shown in Fig. 8.

Firstly, the metering error is measured by the 14-bit A/D converter. Its histogram plot is shown in Fig. 9. It is observed that the metering error can be approximated with triangular-pdf noise. Based on the data, the variance of the current metering error is $V = 1.1218 \times 10^{-4}$. According to (19), the optimal resolution of A/D converter is

$$N_b = \left[\log_2 \frac{I_0}{\sqrt{6V}} + 1\right] = [11.9123] = 12.$$

For comparison, the resolution of the A/D converter is also dropped to 12-bit and 10-bit by software in the following experiments.

In the setup, the target trajectory of motion is shown in Fig. 10. A/D converters with resolution of 10-bit, 12-bit and 14-bit are implemented, respectively. In order to achieve real current signals, two high-precise current probes (Tektronix A622) are also used. The experiment results are shown in Fig. 11∼16. In all these figure, the dashed line shows the results obtained by 10-bit ADC, the solid line shows the results obtained by 12-bit ADC, and the dot-dashed line shows the results obtained by 14-bit one. Fig. 11 shows the comparison of U-phase measured current signals: the signals after the A/D conversion. These signals are used as feedback signals, respectively. Fig. 12 shows the comparison of real current signals (upper part) and the current tracking errors (lower part). The fast-Fourier-transform analysis of the current tracking error is shown in Fig. 13. It is observed that the amplitude of current tracking error is almost the same over whole range of frequencies, which means that the error is whitened. The fast Fourier transform analysis of d,q-axis current are shown in Fig. 14∼15. The position tracking errors are shown in Fig. 16. It is observed that the A/D converter with resolution of 12-bit obtained at least the same performance with 14-bit ADC. The comparison of average tracking error is shown in Table 2. These results also indicate that white noise has smaller effects on control performance compared with other colored noise.

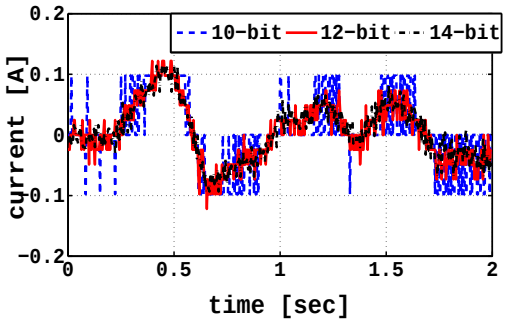

Fig. 11. Comparison of the measured currents (U-phase currents).

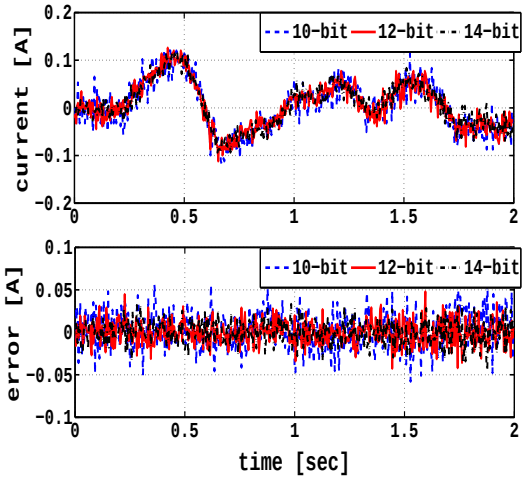

Fig. 12. Comparison of the real U-phase currents (upper) and the current tracking error (lower).

5. Conclusion

In this paper, some significant theorems on quantization and dithering techniques are reviewed. The current measurement for digital current control is analyzed. It is illustrated that by the use of A/D converters having a suitably chosen resolution, the quantization noise can be whitened by the current metering error as well as the variance of total

measurement error is minimized. Based on the view of this point, the optimal resolution of A/D converters can be determined. The effectiveness of this perspective is verified by experiments using a high-precision stage.

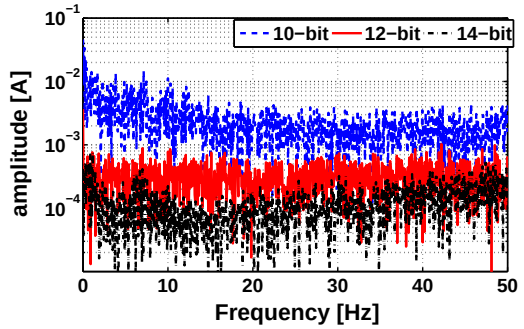

Fig. 13. The FFT analysis of the U-phase currents tracking error.

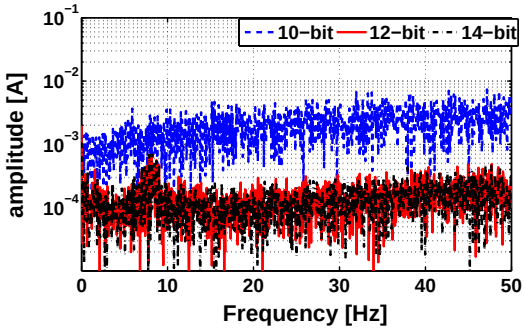

Fig. 14. FFT analysis of the d-axis currents error.

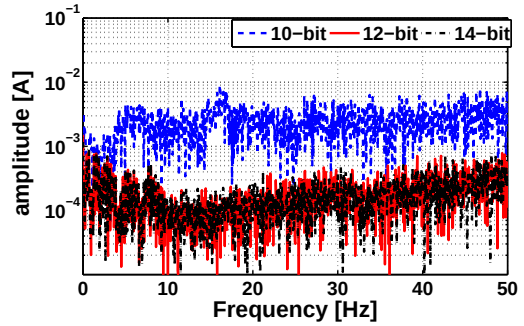

Fig. 15. FFT analysis of the q-axis currents error.

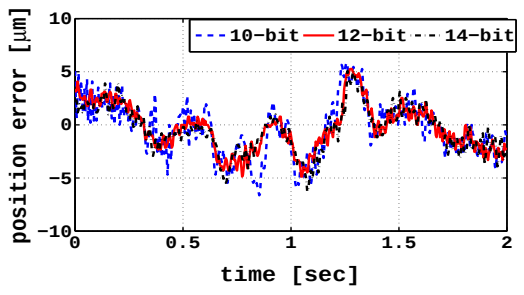

Fig. 16. Comparison of the position tracking error.

Table 2. The RMS of tracking error

	14-bit	12-bit	10-bit
tracking error (μm)	2.1634	2.1485	2.5265

References

(1) D.W. Chung, and S.K. Sul, "Analysis and Compensation of Current Measurement Error in Vector-Controlled AC Motor Drives" *IEEE Trans. Indust. Appl.* , Vol. 34, No. 2, pp. 340–345, Mar./Apr. 1998.

(2) J. Holtz, and J. Quan, "Sensorless Vector Control of Induction Motors at Very Low Speed Using a Nonlinear Inverter Model and Parameter Identification", *IEEE Trans. Indust. appl.* , Vol. 38, No. 4, pp. 1087–1095, Jul./Aug. 2002.

(3) K. Nakamura, H. Fujimoto, and M. Fujisuna, "Torque Ripple Suppression Control for PM Motor Considering the Bandwidth of Torque Meter" (in Japanese), *IEEJ Trans. IA* , Vol. 130, No. 11 pp. 1241–1247, 2010.

(4) J.H. Jang, S.K. Sul, and Y.C. Son, "Current Measurement Issues in Sensorless Control Algorithm using High Frequency Signal Injection Method" *Proc. IEEE Ind. App. Soc. Annual Meeting* , Vol.2 pp. 1134–1141, Oct. Salt Lake City, 2003.

(5) D. Antic, J. B. Klaassens, and W. Deleroi, "Side effects in low-speed AC drives", *Conf. Rec. IEEE-PESC Meeting.* , pp. 998–1002, 1994.

(6) L. Schuchman, "Dither Signals and Their Effect on Quantization Noise", *IEEE Trans. Commun. Technol.* , pp. 162–165, Decr. 1964.

(7) S. P. Lipshitz, R. A. Wannamaker, and J. Vanderkooy, "Quantization and Dither: A Theoretical Survey", *J. Audio Eng. Soc.* , Vol. 40, No.5, pp. 355–375, May 1992.

(8) R. A. Wannamaker, S. P. Lipshitz, J. Vanderkooy,and J. N. Wright, "A Theory of Nonsubtractive Dither", *IEEE Trans. Signal Processing* , Vol. 48, No.2, pp. 499–516, Feb. 2000.

(9) M. F. Wagdy, "Effect of Various Dither Forms on Quantization Errors of Ideal A/D Converters", *IEEE Trans. Instrum. Meas.*, Vol. 38, No.4, pp. 850–855, Aug. 1989.

(10) B. Widrow, "Statistical Analysis of Amplitude-Quantized Sampled-Data Systems", *Trans. AIEE*, Pt. II: Appl. Ind., Vol. 79, pp.555 - 568, 1960.

(11) A. B. Sripad, and D. L. Snyder, "A Necessary and Sufficient Condition for Quantization Errors to be Uniform and White", *IEEE Trans. Acoust., Speech, Signal Processing*, Vol. ASSP-25, No. 5, pp. 442–448, Oct. 1977.

(12) D.W. Chung and S.K. Sui, "Analysis and Compensation of Current Measurement Error in Vector-Controlled AC Motor Drives", *IEEE Trans. Indust. Applicat.* , Vol. 34: No. 2, pp. 340–345, Mar./Apr. 1998.

(13) K. Sakata, H. Fujimoto, "High Bandwidth Design of Feedback Control System Using Multiple Sensors for High-Precision Stage", *Proc. The 39th SICE Symposium on Control Theory* , pp. 285-290, 2010 (in Japanese).